COMPUTATIONAL ASPECTS OF TWO DIFFERENT GEOMETRICALLY NONLINEAR STRUCTURAL TIME DISCRETIZATION MODELS FOR FLUID-STRUCTURE INTERACTION PROBLEMS

Alexandre Luis Braun
Programa de Pós-Graduação em Engenharia Civil (PPGEC)
Universidade Federal do Rio Grande do Sul (UFRGS)
Av. Osvaldo Aranha, 99 – 3° andar, Porto Alegre, RS, Brasil, CEP 90035-190
allbraun@ig.com.br

Abstract. *Computational aspects of two different structural models to be used in fluid-structure interaction simulations are analyzed in this work. Fluid-structure interaction algorithms are employed today to simulate, for example, the wind action over various kinds of structures. These problems are characterized by two different large systems having a highly nonlinear dynamic equilibrium. Although the structural systems usually require a coarse mesh, the same mesh refinement of the fluid domain on the interface is required for the structure when a compatible fluid-structure interface discretization is used. Hence, an efficient structural model able to analyze a geometrically nonlinear dynamic behavior is requested. If an eight-node hexahedral isoparametric finite element with one-point quadrature is used to analyze the fluid domain, it may be convenient to employ the same element type to analyze the structure as a 3-D elastic body (independently if it may be characterized as a thin shell). In order to avoid the excitation of spurious modes an efficient hourglass control technique is used. The shear locking is eliminated by describing the strain tensor in a corotational system. Two different time-marching models for the dynamic equilibrium equation are studied: the Newmark implicit scheme and the explicit Taylor-Galerkin scheme. From previous analyses it was concluded that the Newmark method is much more fast than the Taylor-Galerkin method for small problems. However, the memory required increases considerably for large problems and the Newmark model may become less attractive. Thus, the main objective of this paper, as a first approach towards a fluid-structure algorithm, is to compare these two time discretization methods in a massive meshing condition. Benchmark problems are analyzed in order to evaluate the computational efficiency of the proposed models for large number of degrees of freedom.*

Keywords: *Structural analysis, Geometrically nonlinear dynamics, Finite Element Method (FEM), Volumetric and shear locking control.*

1. Introduction

The numerical simulation of the interaction between fluids and structures plays an important role in many engineering applications. Some examples of application include the wind response of tall buildings, bridges and lightweight roofs, parachute dynamics, flutter prediction in aircrafts and the blood flow through arteries. In all these numerical simulations, realistic models are required to describe the physical problem, which is characterized by a fluid-structure coupled system with a 3-D highly nonlinear dynamic behavior. Although a simple rigid body motion description may be used to represent the structural system *(Braun*, 2002), flexible models with large displacements and/or large deformations are requested by many real world simulations.

An important issue in the fluid-structure interaction algorithms is related to the fluid-structure coupling. In the partitioned (or staggered) procedure, the solution of the coupled problem is accomplished by a separated analysis with different algorithms over the fluid, structure and ALE (Arbitrary Lagrangian-Eulerian) portions of the mesh in a sequential form. On the other hand, in the monolithic approach the primitive variables of the structural dynamic equilibrium equation are the velocity and the stress tensor instead of the classical form with displacements and its derivatives. Consequently, a coupled system can be regarded as a whole once the coupling conditions (velocity compatibility and force equilibrium on the interface) are applied. In both procedures fine fluid mesh discretizations are usually needed in order to correctly represent the fluid flow near immersed bodies. On the other hand, the structural analysis may be perfectly performed with a coarse mesh. However, because of the mesh conformity on the fluid-structure interface, the structural elements are enforced to match the fluid element sizes on this place. Consequently, an efficient structural code is necessary in order to perform the analysis in a massive meshing condition.

Large-scale structural analysis has been a matter of study of many researchers. In the context of the Finite Element Method (FEM), modern algorithms have used one-point quadrature elements to avoid full integration of element matrices. Moreover, classical elements employed in shell and plate structures have been replaced by simple elements, such as the eight-node hexahedral element. Nevertheless, spurious modes may be excited if an efficient stabilization technique (hourglass control) is not employed. In addition, the time discretization method is also very important in the sense to construct an efficient code.

In this work a geometrically nonlinear dynamic model based upon the paper presented by *Duarte Filho and Awruch* (2004) is used. The volumetric locking is eliminated by a reduced-selective integration of the gradient matrix. The shear

locking is avoided by describing the strain rate tensor in a corotational coordinates system. The Newmark implicit scheme and the explicit Taylor-Galerkin scheme are compared in order to obtain the most efficient method to be applied to fluid-structure problems. Very fine meshes are used to analyze classical benchmark problems and perform this comparison. *Duarte Filho and Awruch* (2004) concluded that the Newmark method is much more efficient than the Taylor-Galerkin scheme when coarse meshes are used in the analyses. However, the memory required increases considerably for large problems and the Newmark model may become less attractive. The constitutive equation is given according to the Truesdell rate in order to assure an objective stress rate for the implicit time-marching scheme.

2. The principle of virtual work

The principle of virtual work in the context of the finite element method is given by the following expression (*Belytschko et al*., 2000):

$$\int_{V_e} \delta\mathbf{u}^t \rho \ddot{\mathbf{u}}\, dV + \int_{V_e} \delta\mathbf{u}^t \varphi \dot{\mathbf{u}}\, dV + \delta\mathbf{W}_e^{int} = \int_{V_e} \delta\mathbf{u}^t \mathbf{b}\, dV + \int_{S_e} \delta\mathbf{u}^t \bar{\mathbf{p}}\, dS \tag{1}$$

where ρ is the specific mass, φ is the damping coefficient, $\delta\mathbf{u}$ is the vector of virtual displacements, $\mathbf{u}$ is the vector of displacements, $\dot{\mathbf{u}}$ is the vector of velocity, $\ddot{\mathbf{u}}$ is the vector of acceleration, $\mathbf{b}$ is the vector of body forces, $\bar{\mathbf{p}}$ is the vector of surface load applied on S_e and $\delta\mathbf{W}_e^{int}$ is the vector of internal virtual work, which is expressed by:

$$\delta\mathbf{W}_e^{int} = \int_{V_e} \delta\boldsymbol{\varepsilon}^t \boldsymbol{\sigma}\, dV \tag{2}$$

where $\boldsymbol{\sigma}$ is the stress vector and $\delta\boldsymbol{\varepsilon}$ is the virtual strain vector. It is important to notice that all the values defined above are referred to a generic element *e*.

Displacements, velocities and accelerations are approximated in the finite element method by the nodal values $\mathbf{U}_{(e)}$, $\dot{\mathbf{U}}_{(e)}$ and $\ddot{\mathbf{U}}_{(e)}$ and shape functions N of the element (*e*), as follows:

$$\mathbf{u} = \mathbf{N}\mathbf{U}_{(e)} \quad ; \quad \dot{\mathbf{u}} = \mathbf{N}\dot{\mathbf{U}}_{(e)} \quad ; \quad \ddot{\mathbf{u}} = \mathbf{N}\ddot{\mathbf{U}}_{(e)} \quad ; \quad \delta\mathbf{u} = \mathbf{N}\,\delta\mathbf{U}_{(e)} \tag{3}$$

The strain vector may be approximated in terms of the vector of nodal displacements at element level as follows:

$$\boldsymbol{\varepsilon} = \bar{\mathbf{B}}\mathbf{U}_{(e)} \tag{4}$$

where $\bar{\mathbf{B}}$ is the gradient matrix.

The relation between stress and deformation is given by the elastic constitutive equation, expressed by:

$$\boldsymbol{\sigma} = \mathbf{C}\boldsymbol{\varepsilon} \tag{5}$$

where $\mathbf{C}$ is the elastic constitutive matrix.

Regarding equations (3) and (4), the internal virtual work may be re-written in the following form:

$$\delta\mathbf{W}_e^{int} = \delta\mathbf{U}_{(e)}^t \int_{V_e} \bar{\mathbf{B}}^t \boldsymbol{\sigma}\, dV \tag{6}$$

Equation (1) can be finally expressed in matrix form, which is also called dynamic equilibrium equation:

$$\mathbf{M}\ddot{\mathbf{U}} + \mathbf{D}\dot{\mathbf{U}} + \mathbf{K}\mathbf{U} = \mathbf{P} \tag{7}$$

with:

$$\mathbf{M} = \int_{V_e} \rho \mathbf{N}^t \mathbf{N}\, dV \quad ; \quad \mathbf{D} = \int_{V_e} \varphi \mathbf{N}^t \mathbf{N}\, dV \quad ; \quad \mathbf{K} = \int_{V_e} \bar{\mathbf{B}}^t \mathbf{C} \bar{\mathbf{B}}\, dV \quad ; \quad \mathbf{P} = \int_{V_e} \mathbf{N}^t \mathbf{b}\, dV + \int_{V_e} \mathbf{N}^t \bar{\mathbf{p}}\, dV \tag{8}$$

where $\mathbf{M}$, $\mathbf{D}$ and $\mathbf{K}$ are the mass, damping and stiffness matrices, respectively. $\mathbf{P}$ is the external forces vector.

3. The reduced integration and the stabilizing procedure

Considering a tri-linear isoparametric hexahedral element, spatial coordinates and displacement components are approximated by the following expressions:

$$x_i = \sum_{a=1}^{8} N^a x_i^a \quad (i = 1,2,3) \quad ; \quad u_i = \sum_{a=1}^{8} N^a u_i^a \quad (i = 1,2,3) \tag{9}$$

with the shape functions given by:

$$N^a(\xi,\eta,\zeta) = \frac{1}{8}(1+\xi_a\xi)(1+\eta_a\eta)(1+\zeta_a\zeta) \tag{10}$$

where ξ_a, η_a and ζ_a are the natural coordinates of the node *a* of a generic element.

The one-point quadrature is used in the reduced integration so that the shape functions and its derivatives are evaluated at the center of the element ($\xi = \eta = \zeta = 0$). In order to avoid the volumetric locking a reduced selective integration (*Hughes*, 1980) is performed over the gradient matrix $\overline{\mathbf{B}}$. This matrix is then decomposed as follows:

$$\overline{\mathbf{B}}(\xi,\eta,\zeta) = \tilde{\mathbf{B}}(0) + \hat{\mathbf{B}}(\xi,\eta,\zeta) \tag{11}$$

where $\tilde{\mathbf{B}}(0)$ is the part of the gradient matrix that corresponds to the volumetric part of the strain vector evaluated at the center of the element and $\hat{\mathbf{B}}(\xi,\eta,\zeta)$ is the part of the gradient matrix that corresponds to the deviatoric part of the strain vector.

In addition, $\hat{\mathbf{B}}(\xi,\eta,\zeta)$ must be expanded in Taylor series at the element center up to bilinear terms. Consequently, Eq. (11) can be re-written as:

$$\overline{\mathbf{B}}(\xi,\eta,\zeta) = \mathbf{B}(0) + \hat{\mathbf{B}}_{,\xi}(0)\xi + \hat{\mathbf{B}}_{,\eta}(0)\eta + \hat{\mathbf{B}}_{,\zeta}(0)\zeta + 2\hat{\mathbf{B}}_{,\xi\eta}(0)\xi\eta + 2\hat{\mathbf{B}}_{,\eta\zeta}(0)\eta\zeta + 2\hat{\mathbf{B}}_{,\xi\zeta}(0)\xi\zeta \tag{12}$$

where $\mathbf{B}(0) = \tilde{\mathbf{B}}(0) + \hat{\mathbf{B}}(0)$ is the contribution of the volumetric and deviatoric parts of the gradient matrix obtained from the one-point quadrature.

The stress vector is also expanded in Taylor series in the same manner as it was done above so that:

$$\boldsymbol{\sigma}(\xi,\eta,\zeta) = \boldsymbol{\sigma}(0) + \hat{\boldsymbol{\sigma}}_{,\xi}(0)\xi + \hat{\boldsymbol{\sigma}}_{,\eta}(0)\eta + \hat{\boldsymbol{\sigma}}_{,\zeta}(0)\zeta + 2\hat{\boldsymbol{\sigma}}_{,\xi\eta}(0)\xi\eta + 2\hat{\boldsymbol{\sigma}}_{,\eta\zeta}(0)\eta\zeta + 2\hat{\boldsymbol{\sigma}}_{,\xi\zeta}(0)\xi\zeta \tag{13}$$

By substituting equations. (12) and (13) into Eq. (6), and considering the decomposition given by Eq. (11), the following expression for the internal virtual work at element level is obtained:

$$\begin{aligned}\delta\mathbf{W}_e^{\text{int}} = \delta\mathbf{U}_{(e)}^{\text{t}} \Bigg[& \mathbf{B}^{\text{t}}(0)\boldsymbol{\sigma}(0) + \frac{1}{3}\hat{\mathbf{B}}_{,\xi}^{\text{t}}(0)\hat{\boldsymbol{\sigma}}_{,\xi}(0) + \frac{1}{3}\hat{\mathbf{B}}_{,\eta}^{\text{t}}(0)\hat{\boldsymbol{\sigma}}_{,\eta}(0) + \frac{1}{3}\hat{\mathbf{B}}_{,\zeta}^{\text{t}}(0)\hat{\boldsymbol{\sigma}}_{,\zeta}(0) + \\ & \frac{1}{9}\hat{\mathbf{B}}_{,\xi\eta}^{\text{t}}(0)\hat{\boldsymbol{\sigma}}_{,\xi\eta}(0) + \frac{1}{9}\hat{\mathbf{B}}_{,\eta\zeta}^{\text{t}}(0)\hat{\boldsymbol{\sigma}}_{,\eta\zeta}(0) + \frac{1}{9}\hat{\mathbf{B}}_{,\xi\zeta}^{\text{t}}(0)\hat{\boldsymbol{\sigma}}_{,\xi\zeta}(0) \Bigg] V_{(e)}\end{aligned} \tag{14}$$

where $V_{(e)}$ is the volume of the element (e).

The internal force vector at element level may be expressed by:

$$\mathbf{f}^{\text{int}} = \mathbf{f}^{\text{e}} + \mathbf{f}^{\text{hg}} = (\mathbf{K}^{\text{e}} + \mathbf{K}^{\text{stab}})\mathbf{U} = \mathbf{K}\mathbf{U} \tag{15}$$

where:

$$\mathbf{f}^{\text{e}} = \mathbf{B}^{\text{t}}(0)\boldsymbol{\sigma}(0)V_e \Big[\mathbf{B}^{\text{t}}(0)\mathbf{C}\mathbf{B}(0)V_e\Big]\mathbf{U} = \mathbf{K}^{\text{e}}\mathbf{U} \tag{16}$$

which corresponds to the one-point quadrature part of the internal force vector and:

$$\begin{aligned}\mathbf{f}^{\text{hg}} = \mathbf{K}^{\text{stab}}\mathbf{U} = \Bigg[& \frac{1}{3}\hat{\mathbf{B}}_{,\xi}^{\text{t}}(0)\hat{\boldsymbol{\sigma}}_{,\xi}(0) + \frac{1}{3}\hat{\mathbf{B}}_{,\eta}^{\text{t}}(0)\hat{\boldsymbol{\sigma}}_{,\eta}(0) + \frac{1}{3}\hat{\mathbf{B}}_{,\zeta}^{\text{t}}(0)\hat{\boldsymbol{\sigma}}_{,\zeta}(0) + \\ & \frac{1}{9}\hat{\mathbf{B}}_{,\xi\eta}^{\text{t}}(0)\hat{\boldsymbol{\sigma}}_{,\xi\eta}(0) + \frac{1}{9}\hat{\mathbf{B}}_{,\eta\zeta}^{\text{t}}(0)\hat{\boldsymbol{\sigma}}_{,\eta\zeta}(0) + \frac{1}{9}\hat{\mathbf{B}}_{,\xi\zeta}^{\text{t}}(0)\hat{\boldsymbol{\sigma}}_{,\xi\zeta}(0) \Bigg] V_{(e)}\end{aligned} \tag{17}$$

which corresponds to the hourglass control part of the internal force vector. The stress-strain constitutive relations for the first and second derivatives of the stress vector given in Eq. (17) are obtained as follows:

$$\hat{\boldsymbol{\sigma}}_{,\xi} = \mathbf{E}\hat{\boldsymbol{\varepsilon}}_{,\xi} \quad ; \quad \hat{\boldsymbol{\sigma}}_{,\eta} = \mathbf{E}\hat{\boldsymbol{\varepsilon}}_{,\eta} \quad ; \quad \hat{\boldsymbol{\sigma}}_{,\zeta} = \mathbf{E}\hat{\boldsymbol{\varepsilon}}_{,\zeta} \quad ; \quad \hat{\boldsymbol{\sigma}}_{,\xi\eta} = \mathbf{E}\hat{\boldsymbol{\varepsilon}}_{,\xi\eta} \quad ; \quad \hat{\boldsymbol{\sigma}}_{,\eta\zeta} = \mathbf{E}\hat{\boldsymbol{\varepsilon}}_{,\eta\zeta} \quad ; \quad \hat{\boldsymbol{\sigma}}_{,\xi\zeta} = \mathbf{E}\hat{\boldsymbol{\varepsilon}}_{,\xi\zeta} \tag{18}$$

where $\mathbf{E}$ is the stabilization matrix, proposed by *Hu and Nagy* (1997), which is given by:

$$\mathbf{E} = \begin{bmatrix} \underset{\sim}{\mathrm{e}} & \underset{\sim}{0} \\ \underset{\sim}{0} & \underset{\sim}{\mathrm{e}} \end{bmatrix} \quad ; \quad \mathbf{e} = \begin{bmatrix} 2\mu & 0 & 0 \\ 0 & 2\mu & 0 \\ 0 & 0 & 2\mu \end{bmatrix} \tag{19}$$

where μ is the Lamé constant.

In order to remove the shear locking, the shear components of the strain tensor must be written in an orthogonal corotational coordinates system. In addition, each of the shear components must be linearly interpolated in a single coordinate direction of the reference system. Hence:

$$\begin{aligned} &\hat{\mathbf{B}}_{xy,\xi}(0) = \hat{\mathbf{B}}_{xy,\eta}(0) = \hat{\mathbf{B}}_{xy,\xi\eta}(0) = \hat{\mathbf{B}}_{xy,\eta\zeta}(0) = \hat{\mathbf{B}}_{xy,\xi\zeta}(0) = 0 \\ &\hat{\mathbf{B}}_{yz,\eta}(0) = \hat{\mathbf{B}}_{yz,\zeta}(0) = \hat{\mathbf{B}}_{yz,\xi\eta}(0) = \hat{\mathbf{B}}_{yz,\eta\zeta}(0) = \hat{\mathbf{B}}_{yz,\xi\zeta}(0) = 0 \\ &\hat{\mathbf{B}}_{xz,\xi}(0) = \hat{\mathbf{B}}_{xz,\zeta}(0) = \hat{\mathbf{B}}_{xz,\xi\eta}(0) = \hat{\mathbf{B}}_{xz,\eta\zeta}(0) = \hat{\mathbf{B}}_{xz,\xi\zeta}(0) = 0 \end{aligned} \tag{20}$$

The internal force vector will not be adequately evaluated for distorted element if the one-point quadrature is used. In order to correct this deficiency the gradient matrix obtained with reduced integration $\mathbf{B}(0)$ must be replaced by the uniform gradient matrix $\mathbf{B}'(0)$ defined by *Flanagan and Belytschko* (1983):

$$\mathbf{B}'_{\text{a}}(0) = \frac{1}{V_e}\int_{V_e} \mathbf{B}_{\text{a}}(\xi,\eta,\zeta)\,\text{dV} \quad (\text{a} = 1,...,8) \tag{21}$$

where *a* corresponds to the node number of the element *e*.

4. The geometrically nonlinear analysis with the corotational reference system

In order to avoid the shear locking, it is also necessary to employ a corotational coordinates system for the geometric description, where the reference system is attached to the local coordinates system of the finite element.

The motion of a continuous medium may be decomposed into rigid body motion and a pure deformation. Since the spatial discretization of the problem is fine enough, this decomposition can be performed at element level, and consequently in the corotational system, where the pure deformation portion will always be a small quantity relative to the element dimensions.

To calculate stress and strain updates, it is necessary to evaluate the deformation part of the displacement field in the corotational system. The displacement field, in an incremental form, can be separated into a part owing to pure deformations and a part owing to pure rotations, similarly to polar decomposition, as follows:

$$\Delta\mathbf{u} = \Delta\mathbf{u}^{\text{def}} + \Delta\mathbf{u}^{\text{rot}} \tag{22}$$

where $\Delta\mathbf{u}^{\text{def}}$ and $\Delta\mathbf{u}^{\text{rot}}$ are incremental displacement vectors representing the pure deformation and the pure rotation contributions to the incremental displacement field in the global coordinates system, respectively. The incremental displacement due to pure rotation may be obtained from:

$$\Delta\mathbf{u}^{\text{rot}} = \Delta\mathbf{u} - \mathbf{R}^{\text{t}}_{\text{n+1/2}}\left(\hat{\mathbf{x}}_{\text{n+1}} - \hat{\mathbf{x}}_{\text{n}}\right) \tag{23}$$

where $\mathbf{R}^{\text{t}}_{\text{n+1/2}}$ is the transpose of the orthogonal transformation matrix $\mathbf{R}_{\text{n+1/2}}$, which rotates the global coordinate system to the corresponding corotational coordinates system. This matrix is referred to the mid-point of the time interval [t_n, t_{n+1}] and it is defined from the geometric configuration at this point. $\hat{\mathbf{x}}_{\text{n}}$ and $\hat{\mathbf{x}}_{\text{n+1}}$ are, respectively, the geometric configurations at $t = t_n$ and $t = t_{n+1}$ defined in the corotational coordinates system. They are obtained from the following transformations:

$$\hat{\mathbf{x}}_{\text{n}} = \mathbf{R}_{\text{n}}\mathbf{x}_{\text{n}} \quad ; \quad \hat{\mathbf{x}}_{\text{n+1}} = \mathbf{R}_{\text{n+1}}\mathbf{x}_{\text{n+1}} \tag{24}$$

where $\mathbf{R}_n$ and $\mathbf{R}_{n+1}$ are the transformation matrices defined at $t = t_n$ and $t = t_{n+1}$, respectively. $\mathbf{x}_n$ and $\mathbf{x}_{n+1}$ are the geometric configurations at $t = t_n$ and $t = t_{n+1}$ defined in the global coordinates system, respectively. The deformation displacement increment in the corotational system is finally obtained by the expression:

$$\Delta\hat{\mathbf{u}}^{\text{def}} = \mathbf{R}_{\text{n+1/2}}\Delta\mathbf{u}^{\text{def}} = \hat{\mathbf{x}}_{\text{n+1}} - \hat{\mathbf{x}}_{\text{n}} \tag{25}$$

The components of the transformation matrix are given by:

$$\mathbf{R}_{1\text{j}} = \frac{\mathbf{r}_{1\text{j}}}{\mathbf{r}_1^{\text{t}}\mathbf{r}_1} \quad ; \quad \mathbf{R}_{2\text{j}} = \frac{(\mathbf{r}_{2\text{j}} + \mathbf{r}_{\text{cj}})}{(\mathbf{r}_{2\text{j}} + \mathbf{r}_{\text{cj}})^{\text{t}}(\mathbf{r}_{2\text{j}} + \mathbf{r}_{\text{cj}})} \quad ; \quad \mathbf{R}_{3\text{j}} = \frac{\mathbf{r}_{3\text{j}}}{\mathbf{r}_3^{\text{t}}\mathbf{r}_3} \quad (\text{j} = 1,2,3) \tag{26}$$

with

$$\mathbf{r}_{1\text{j}} = \xi^{\text{t}}\mathbf{x}_{\text{j}} \quad ; \quad \mathbf{r}_{2\text{j}} = \eta^{\text{t}}\mathbf{x}_{\text{j}} \quad ; \quad \mathbf{r}_{\text{cj}} = -\frac{\mathbf{r}_{1\text{j}}^{\text{t}}\mathbf{r}_{2\text{j}}}{\mathbf{r}_{1\text{j}}^{\text{t}}\mathbf{r}_{1\text{j}}}\mathbf{r}_{1\text{j}} \quad ; \quad \mathbf{r}_{3\text{j}} = \mathbf{r}_{1\text{j}} \times (\mathbf{r}_{2\text{j}} + \mathbf{r}_{\text{cj}}) \tag{27}$$

where $\mathbf{x}_j$ is the vector of global coordinates of the nodes of a generic element.

The strain increment is given by the mid-point integration of the velocity strain tensor. It is then written as follows:

$$\Delta\hat{\boldsymbol{\varepsilon}} = \frac{1}{2}\left[\frac{\partial\Delta\hat{\mathbf{u}}^{\text{def}}}{\partial\hat{\mathbf{x}}_{\text{n+1/2}}} + \left(\frac{\partial\Delta\hat{\mathbf{u}}^{\text{def}}}{\partial\hat{\mathbf{x}}_{\text{n+1/2}}}\right)^{\text{t}}\right] \tag{28}$$

The corotational Cauchy tensor is used as the stress measure since it is an objective tensor in this coordinate system. However, the rate of the Cauchy tensor is not objective. Hence, the Truesdell rate is employed in this work, which is given by:

$$\Delta\sigma_{\text{ij}} = \left(\text{C}_{\text{ijkl}} + \hat{\text{C}}_{\text{ijkl}}\right)\Delta\varepsilon_{\text{kl}} + \text{W}_{\text{ijkl}}\Delta\omega_{\text{kl}} \quad (\text{i, j, k, l} = 1,2,3) \tag{29}$$

where

$$\hat{\text{C}}_{\text{ijkl}} = -\sigma_{\text{ij}}\delta_{\text{kl}} + \frac{1}{2}\left(\sigma_{\text{il}}\delta_{\text{jk}} + \sigma_{\text{jl}}\delta_{\text{ik}} + \sigma_{\text{ik}}\delta_{\text{jl}} + \sigma_{\text{jk}}\delta_{\text{il}}\right) \tag{30}$$

and

$$\text{W}_{\text{ijkl}} = \frac{1}{2}\left(\sigma_{\text{il}}\delta_{\text{jk}} + \sigma_{\text{jl}}\delta_{\text{ik}} - \sigma_{\text{ik}}\delta_{\text{jl}} - \sigma_{\text{jk}}\delta_{\text{il}}\right) \tag{31}$$

5. Time-marching schemes for the dynamic analysis

5.1. The Nemark implicit scheme

The dynamic equilibrium equation (Eq. 7) may be presented in an incremental form according to:

$$\mathbf{M}\Delta\ddot{\mathbf{U}} + \mathbf{D}\Delta\dot{\mathbf{U}} + \mathbf{K}^{t}\Delta\mathbf{U} = \mathbf{P}^{t+\Delta t} - \left[\mathbf{M}\ddot{\mathbf{U}} + \mathbf{D}\dot{\mathbf{U}} + \mathbf{f}^{\mathbf{int}}(\mathbf{U})\right]^{t} \tag{32}$$

where all terms were previously defined in Section 2. The implicit Newmark scheme is applied in the time discretization of Eq. (32). Additional information about the method may be found in *Bathe* (1996).

The numerical algorithm employed in the dynamic analysis using the Newmark scheme may be summarized as below:

1. Solve $\Delta\mathbf{U} = \left[\bar{\mathbf{K}}^{-1}\right]^{t}\bar{\mathbf{P}}^{t+\Delta t}$, with $\bar{\mathbf{K}}^{t} = \mathbf{K}^{t} + a_0\mathbf{M} + a_1\mathbf{C}$ and $\bar{\mathbf{P}}^{t+\Delta t} = \mathbf{P}^{t+\Delta t} - \left[\mathbf{M}\ddot{\mathbf{U}} + \mathbf{D}\dot{\mathbf{U}} + \mathbf{f}^{\mathbf{int}}(\mathbf{U})\right]^{t} + \mathbf{M}(a_2\dot{\mathbf{U}} + a_3\ddot{\mathbf{U}})^{t} + \mathbf{D}(a_4\dot{\mathbf{U}} + a_5\ddot{\mathbf{U}})^{t}$
2. Update displacement, velocity and acceleration vectors.
3. Compute the residual load vector $\mathbf{Q}^{t+\Delta t} = \mathbf{P}^{t+\Delta t} - \left[\mathbf{M}\ddot{\mathbf{U}} + \mathbf{D}\dot{\mathbf{U}} + \mathbf{f}^{\mathbf{int}}(\mathbf{U})\right]^{t+\Delta t}$
4. Check convergence: if $\left\|\mathbf{Q}^{t+\Delta t}\right\| / \left\|\mathbf{P}^{t+\Delta t}\right\| \le \mathrm{TOL}$ go to the next time step (1), else go to (5).
5. Compute $\delta\mathbf{U} = \left[\bar{\mathbf{K}}^{-1}\right]^{t}\mathbf{Q}^{t+\Delta t}$
6. Update displacements, velocity and acceleration vector using (5).
7. Compute the residual load vector (step 3) with the new state of motion.
8. Check convergence: if $\left\|\mathbf{Q}^{t+\Delta t}\right\| / \left\|\mathbf{P}^{t+\Delta t}\right\| \le \mathrm{TOL}$ go to the next time step (1), else go to (5).

In the expressions above, a_0, a_1, a_2, a_3, a_4 and a_5 are constants of the Newmark method and they are obtained from the parameters α and δ. In the present work, it was considered $\alpha = 0.25$ and $\delta = 0.5$. TOL is a tolerance criterion. It is important to notice that although the implicit Newmark method is unconditionally stable for linear problems, this feature may be not observed for nonlinear analyses.

5.2. The Taylor-Galerkin explicit scheme

The dynamic equilibrium equation is initially transformed to the following expression (*Duarte Filho and Awruch*, 2004):

$$\frac{\partial\rho\mathbf{v}}{\partial t} - \frac{\partial}{\partial x_j}\mathbf{S}_j + \mathbf{Q} = \mathbf{0} \quad (j = 1,2,3) \tag{33}$$

with

$$\mathbf{v}^{t} = \left[v_1, v_2, v_3\right] \;\; ; \;\; \mathbf{S}_j^{t} = \left[\sigma_{1j}, \sigma_{2j}, \sigma_{3j}\right] \;\; ; \;\; \mathbf{Q}^{t} = \left[\frac{\varphi}{\rho}(\rho v_1) - b_1, \frac{\varphi}{\rho}(\rho v_2) - b_2, \frac{\varphi}{\rho}(\rho v_3) - b_3\right] \tag{34}$$

where φ is the damping coefficient, ρ is the specific mass, b_i are the body force vector components, v_i are the velocity vector components and σ_{ij} are the stress tensor components.

The explicit Taylor-Galerkin model is obtained by expanding Eq. (33) in a Taylor series up to second order terms. By applying the classical Petrov-Galerkin method in the context of the Finite Element Method, the following expression is then obtained:

$$\mathbf{V}^{t+\Delta t} = \mathbf{V}^{t} - \frac{\Delta t}{\psi}\mathbf{M}_{\mathrm{D}}^{-1}\mathbf{H} \tag{35}$$

with

$$\mathbf{H} = \left[\mathbf{f}^{\mathrm{int}} + \mathbf{P}\right]^{t+\Delta t/2} - \frac{\varphi}{\rho}\mathbf{M}_{\mathrm{D}}\mathbf{V}^{t} \tag{36}$$

where $\mathbf{f}^{\mathrm{int}}$ is the vector of elastic forces, $\mathbf{P}$ is the load vector, $\mathbf{V}$ is the vector of nodal velocity, $\mathbf{M_D}$ is the lumped mass matrix and $\psi = 1 + \varphi\Delta t/2\rho$. The explicit scheme is conditionally stable and the following condition must be satisfied:

$$\Delta t \le \Delta t_{\mathrm{crit}} = \lambda\frac{\Delta x}{\sqrt{E\beta/\rho}} \quad \text{with} \quad \beta = \frac{1}{1 - 2\nu^2/(1-\nu)} \tag{37}$$

where λ is a safety coefficient ($\lambda < 1$), Δx is the characteristic dimension of the finite element, E is the Young Modulus and ν is the Poisson coefficient.

6. Numerical applications

Numerical examples are presented in this section in order to compare the different time discretization models employed in this paper for the solution of geometrically nonlinear dynamic problems. The first example considers the dynamic nonlinear response of a 2-D clamped beam under a constant vertical load applied at the mid point of the beam. In the second application the nonlinear dynamic analysis of a 2-D clamped arch with a constant vertical load at its mid-span is performed. In the last problem it is considered the nonlinear dynamic behavior of a simply supported rectangular

plate subjected to a concentrated load applied at its central point. A step function is used for the load on the plate, which varies from zero to the maximum value in 0.006 seconds linearly.

Geometrical characteristics of the numerical examples analyzed in this work are shown in Fig. 1 and its respective numerical values are: for the clamped beam – L = 20 m, h = 0.125 m and P = 640 N; for the clamped arch – R = 100 m, h = 2 m, θ = 0.707 rad and P = 7500 N; for the rectangular plate – a = 1.016 m, b = 1.524 m, h = 0.0254 m and P = 44.54 N. In the clamped beam, clamped arch and rectangular plate analyses the finite element meshes were constituted by (1400x9x1), (920x13x1) and (16x32x4) elements, respectively.

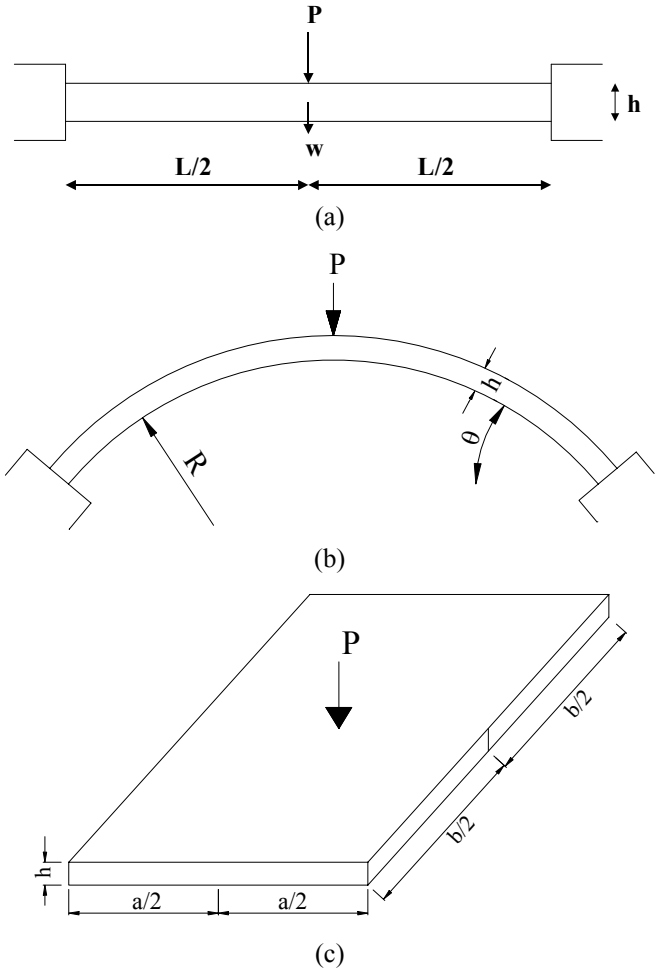

Figure 1. Geometrical characteristics: (a) clamped beam, (b) clamped arch and (c) rectangular plate

The time steps adopted by the Taylor-Galerkin scheme are given according to the stability condition, Eq. 37, with a safety coefficient $\lambda = 0.5$. Consequently, the following values were used: $\Delta t = 1.0 \times 10^{-8}$ s for the clamped beam, $\Delta t = 3.0 \times 10^{-7}$ s for the clamped arch and $\Delta t = 1.0 \times 10^{-5}$ s for the plate. On the other hand, the time increments employed by the Newmark method are chosen such that frequency and period of the structure be well defined. The values used by the Newmark scheme are: $\Delta t = 4.0 \times 10^{-5}$ s for the clamped beam, $\Delta t = 3.0 \times 10^{-5}$ s for the clamped arch and $\Delta t = 1.0 \times 10^{-3}$ s for the plate.

The material properties employed in the present study are given as follows; for the clamped beam: $\rho = 2.45 \times 10^{-4}$ Kg/m^3, $\varphi = 0.0$, $\nu = 0.0$ and $E = 3.0 \times 10^7$ N/m^2; for the clamped arch: $\rho = 2.45 \times 10^{-4}$ Kg/m^3, $\varphi = 0.0$, $\nu = 0.25$ and $E = 3.0 \times 10^7$ N/m^2; and for the rectangular plate: $\rho = 3210.05$ Kg/m^3, $\varphi = 0.0$, $\nu = 0.25$ and $E = 2.095 \times 10^8$ N/m^2.

The dynamic responses obtained by the present work representing the displacements history at the respective load points are plotted in Fig 2. Comparing the results with other numerical references a very good agreement can be observed. Moreover, it is verified that the Newmark and Taylor-Galerkin methods present the same accuracy level in most of the running time.

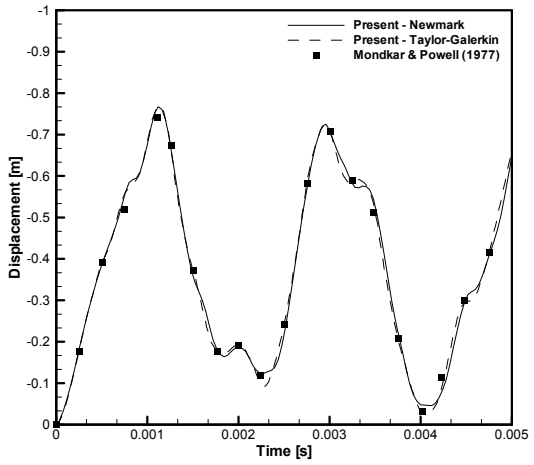

(a)

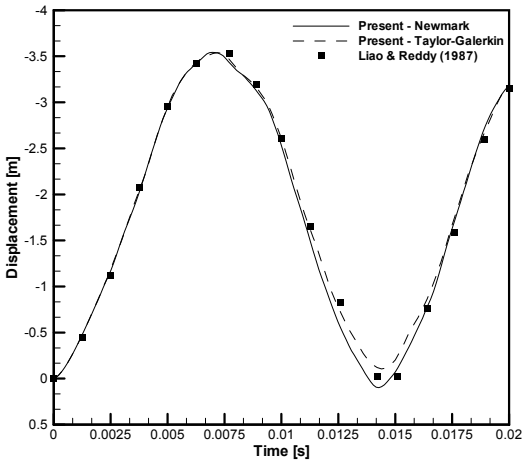

(b)

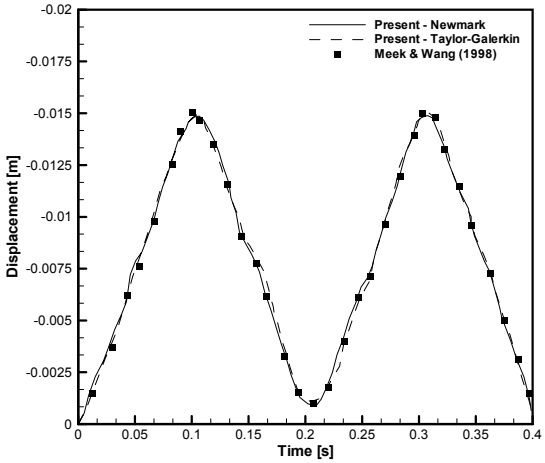

(c)

Figure 2. Displacement time histories according to the numerical example: (a) clamped beam, (b) clamped arch and (c) rectangular plate

The deformed configuration of the rectangular plate at a moment corresponding to its maximum deflection is presented in Fig. 3.

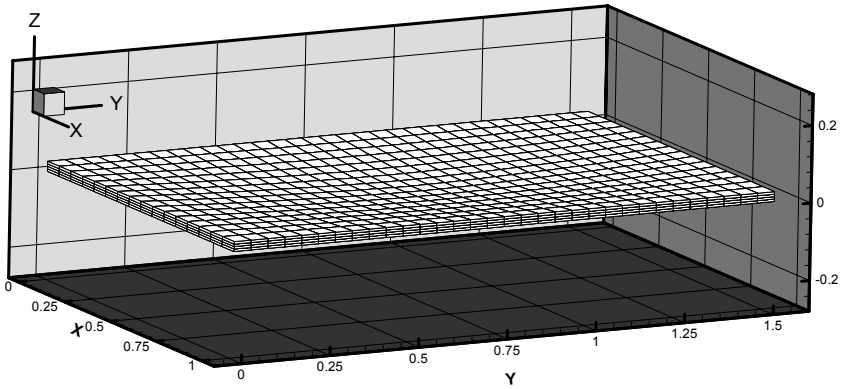

Figure 3. Deformed configuration of the rectangular plate

Information about the computational performance obtained in the numerical examples by the time discretization models presented in this work are summarized in Tab. 1. Results are compared in terms of running time (CPUT), memory used (MEM), running time per time increment (CPUT/I**)**, band-width (B-W) and number of iterations in the incremental process (ITER). It is important to notice that the running time (CPUT) is normalized by the corresponding processing time obtained by the Taylor-Galerkin scheme (*). It is verified that the Newmark method was faster than the Taylor-Galerkin model in all simulations. On the other hand, the Taylor-Galerkin scheme is much more efficient in

terms of the time spent in each time step. In addition, it is observed that the amount of memory requested by the Taylor-Galerkin method is about five times smaller than the amount of memory employed by the Newmark scheme. The number of iterations of the incremental process to solve the dynamic equation using the Newmark method is related to time step chosen to perform the analysis. The higher is this value the higher is the number of iterations. The band-width is also an important aspect related to the numerical efficiency of the Newmark method. It is concluded that a large band-width may deteriorate the efficiency of the model, as it is observed in the rectangular plate analysis.

Table 1. Computational performance of the numerical models

Model	Example	CPUT	MEM [Mw]†	CPUT/I	B-W	ITER
Newmark	Clamped beam	0.285*[1]	21.61	39.41	102	5
	Clamped arch	0.539*[2]	20.51	66.01	138	4
	Rectangular plate	0.880*[3]	3.60	21.78	420	3.4
Taylor-Galerkin	Clamped beam	1*[1]	4.05	0.09	–	–
	Clamped arch	1*[2]	4.33	1.22		
	Rectangular plate	1*[3]	0.76	0.247		

† - *1 w = 8 bytes*

7. Conclusions

The main objective of the present work was the determination of the most efficient numerical procedure to analyze geometrically nonlinear structures with large number of unknowns, namely, fluid-structure interaction problems. It was verified that the Taylor-Galerkin method is a very efficient scheme in terms of the time dispended in each time step. However, the stability condition imposed to explicit time-marching algorithms leads to a very restrictive time increment, mainly for nonlinear structural analyses. Hence, the method is mostly indicated for parallel computation environments and highly transient problems, when the natural time scale of the problem is inherently small. On the other hand, the Newmark method proved to be a better solver even in a massive meshing condition. It was expected that the increase in the memory requirements could become the Newmark scheme less attractive when it is compared to the Taylor-Galerkin method. Nevertheless, it was concluded that once the band-width is optimized, the method is more efficient than the Taylor-Galerkin model in most situations.

8. Acknowledgements

The author wishes to thank to CNPq by the financial support.

9. References

Bathe, K. J., 1996, “Finite Element Procedures”, Prentice Hall, Englewood Cliffs, NJ.

Belytschko, T., Liu, W.K. and Moran, B., 2000, “Nonlinear Finite Elements for Continua and Structures”, John Willey & Sons, West Sussex, England.

Braun, A.L., 2002, “A Numerical Model for the Simulation of the Wind Action over Bridge Cross-Sections” (In Portuguese), MSc Thesis, Graduate Program in Civil Engineering / Federal University of Rio Grande do Sul (PPGEC/UFRGS), Porto Alegre, Brazil.

Duarte Filho, L. A. and Awruch, A. M., 2004, “Geometrically nonlinear static and dynamic analysis of shells and plates using the eight-node hexahedral element with one-point quadrature”, Finite Elements in Analysis and Design, vol. 40, pp. 1297-1315.

Flanagan, D.P. and Belytschko, T., 1983, “A uniform strain hexahedron and quadrilateral with orthogonal hourglass control”, International Journal of Numerical Methods in Engineering, vol. 17, pp. 679-706.

Hughes, T.J., 1980, “Generalization of selective integration procedures to anisotropic and nonlinear media”, International Journal of Numerical Methods in Engineering, vol. 15, pp. 1413-1418.

Hu, Y.K. and Nagy, L.I., 1997, “A one-point quadrature eight-node brick element with hourglass control. Computers & Structures”, vol. 65, pp. 893-902.

Liao, C. and Reddy, J.N., 1987, “An incremental total Lagrangean formulation for general anisotropic shell-type structures”, Research Report n° VPII-E-87.22, Dept. of Engineering Science and Mechanics, Virginia Polytechnic Institute, State University, Virginia (USA).

Meek, J.L. and Wang, Y., 1998, “Nonlinear static and dynamic analysis of shell structures with finite rotation”, Computational Methods in Applying Mechanics and Engineering, vol. 162, pp. 301-315.

Mondkar, D.P. and Powell, G.H., 1977, “Finite element analysis of nonlinear static and dynamic response”, International Journal for Numerical Methods in Engineering, vol. 11, pp. 499-520.

10. Responsibility notice

The author is the only responsible for the printed material included in this paper.